












Evolutionarily distinct resistance proteins detect a pathogen effector through its association with different host targets

Haixia Wang^{1,2} , Franziska Trusch¹ , Dionne Turnbull¹ , Carolina Aguilera-Galvez³, Susan Breen^{4,5} , Shaista Naqvi¹ , Jonathan D. G. Jones⁶ , Ingo Hein^{1,4} , Zhendong Tian² , Vivianne Vleeshouwers³ , Eleanor Gilroy⁴  and Paul R. J. Birch^{1,4} 

¹Division of Plant Sciences, University of Dundee, At James Hutton Institute, Errol Rd, Invergowrie, Dundee, DD2 5DA, UK; ²Key Laboratory of Horticultural Plant Biology (HZAU), Ministry of Education, Key Laboratory of Potato Biology and Biotechnology (HZAU), Ministry of Agriculture and Rural Affairs, Huazhong Agricultural University, Wuhan, Hubei 430070, China; ³Plant Breeding, Wageningen University and Research, Droevendaalsesteeg 1, Wageningen 6708 PB, the Netherlands; ⁴Cell and Molecular Sciences, James Hutton Institute, Errol Road, Invergowrie, Dundee, DD2 5DA, UK; ⁵School of Life Sciences, The University of Warwick, Gibbet Hill Campus, Coventry, CV4 7AL, UK; ⁶The Sainsbury Laboratory, Norwich Research Park, Norwich, NR4 7UH, UK

Summary

Author for correspondence:
Paul R. J. Birch
Email: Paul.Birch@hutton.ac.uk

Received: 8 May 2021
Accepted: 26 July 2021

New Phytologist (2021) 232: 1368–1381
doi: 10.1111/nph.17660

Key words: avirulence, cell death, effector-triggered immunity, NLR, plant immunity, plant pathogen co-evolution, potato late blight, resistance protein.

- Knowledge of the evolutionary processes which govern pathogen recognition is critical to understanding durable disease resistance. We determined how *Phytophthora infestans* effector *PiAVR2* is recognised by evolutionarily distinct resistance proteins R2 and Rpi-mcq1.
- We employed yeast two-hybrid, co-immunoprecipitation, virus-induced gene silencing, transient overexpression, and phosphatase activity assays to investigate the contributions of BSL phosphatases to R2- and Rpi-mcq1-mediated hypersensitive response (R2 HR and Rpi-mcq1 HR, respectively).
- Silencing *PiAVR2* target *BSL1* compromises R2 HR. Rpi-mcq1 HR is compromised only when *BSL2* and *BSL3* are silenced. *BSL1* overexpression increases R2 HR and compromises Rpi-mcq1. However, overexpression of *BSL2* or *BSL3* enhances Rpi-mcq1 and compromises R2 HR. Okadaic acid, which inhibits BSL phosphatase activity, suppresses both recognition events. Moreover, expression of a *BSL1* phosphatase-dead (PD) mutant suppresses R2 HR, whereas *BSL2*-PD and *BSL3*-PD mutants suppress Rpi-mcq1 HR. R2 interacts with *BSL1* in the presence of *PiAVR2*, but not with *BSL2* and *BSL3*, whereas no interactions were detected between Rpi-mcq1 and BSLs. Thus, *BSL1* activity and association with R2 determine recognition of *PiAVR2* by R2, whereas *BSL2* and *BSL3* mediate Rpi-mcq1 perception of *PiAVR2*.
- R2 and Rpi-mcq1 utilise distinct mechanisms to detect *PiAVR2* based on association with different BSLs, highlighting central roles of these effector targets for both disease and disease resistance.

Introduction

Plant pathogens secrete an array of effector proteins into host cells to suppress pattern-triggered immunity (PTI), which is activated following the perception of microbe-associated molecular patterns (MAMPs) by pattern recognition receptors (PRRs) at the host plasma membrane (Jones & Dangl, 2006). In turn, plants possess resistance (R) proteins to directly or indirectly detect corresponding effectors, which are consequently called avirulence (AVR) proteins, leading to the activation of effector-triggered immunity (ETI). Effector-triggered immunity often involves a rapid, localized host cell death (CD) known as the hypersensitive response (HR) (Jones & Dangl, 2006). A detailed understanding of the recognition of effectors and their coevolution with cognate R proteins underpins our knowledge of plant immunity and can inform us as to how best to deploy effective

disease resistance in crops. Nucleotide binding leucine-rich repeat or NOD-like receptor (NLR) proteins are the largest family of R proteins (Eitas & Dangl, 2010; Elmore *et al.*, 2011; Jones *et al.*, 2016). They can either directly interact with cognate AVR effectors, or indirectly recognize AVRs based on their activities and their targets (Khan *et al.*, 2016). Due to increasing efforts to identify and characterise effector targets, our understanding of how NLRs and their targets evolve to enable detection of recognized effectors is steadily expanding.

The yield and quality of potato (*Solanum tuberosum*), the third most important global food crop, is threatened by many devastating diseases (Hayward, 1991; Stevenson, 1994; Birch *et al.* 2012; Liu *et al.*, 2016). Chief among them is late blight, caused by the oomycete pathogen *Phytophthora infestans*. Significant progress has been made in the identification and cloning of NLRs that confer resistance to *P. infestans* (*Rpi*) from diverse wild

potato species. Mexico is a centre of diversity of *Rpi* genes, including *R1-R11*, *Rpi-blb1/2/3*, *Rpi-sto1*, *Rpi-pta*, *Rpi-mcb1*, *Rpi-ver1* and *Rpi1* from *Solanum demissum*, *Solanum bulbocastanum*, *Solanum stoloniferum*, *Solanum papita*, *Solanum michoacanum*, *Solanum verrucosum* and *Solanum pinnatisectum*, respectively (Kuhl *et al.*, 2001; Hein *et al.*, 2009; Vleeshouwers *et al.*, 2011; Śliwka *et al.*, 2012a; de Vetten *et al.*, 2014; Jo *et al.*, 2015; Van Weymers *et al.*, 2016; Chen *et al.*, 2018). South America is a second source of *Rpi* genes, including *Rpi-mcq1*, *Rpi-vnt1*, *Rpi-ber*, *Rpi-chc1*, *Rpi-tar1* and *Rpi-rzc1* from *Solanum mochiquense*, *Solanum venturii*, *Solanum berthaultii*, *Solanum chacoense*, *Solanum tarijense* and *Solanum ruiz-ceballosii* respectively (Smilde *et al.*, 2005; Jones *et al.*, 2007; Foster *et al.*, 2009; Park *et al.*, 2009; Pel *et al.*, 2009; Vossen *et al.*, 2009; Śliwka *et al.*, 2012b; Jones *et al.*, 2014).

The NLR R2 belongs to a highly diverse gene family that is native to Mexican *Solanum* species, and resides in a major late blight resistance locus on chromosome IV of *S. demissum* (Li *et al.*, 1998; Park *et al.*, 2005a,b,c; Lokossou *et al.*, 2009). It recognizes the *P. infestans* effector PiAVR2 (Gilroy *et al.*, 2011), which belongs to a family of sequence-divergent *P. infestans* RXLR effectors (Champouret, 2010). PiAVR2 accumulates at sites of *P. infestans* haustorial penetration during infection and interacts with potato and tomato phosphatase BRI1-SUPPRESSOR1-like 1 (BSL1) (Saunders *et al.*, 2012). BSL1 is a protein phosphatase and belongs to the BSU1 (BRI1 SUPPRESSOR1) family (BSUf; BSU1, BSL1, BSL2 and BSL3), which is thought to contribute to brassinosteroid (BR) signalling (Mora-García *et al.*, 2004; Kim *et al.*, 2009). BSL1 interaction with PiAVR2 is required for R2-mediated HR (R2 HR) (Saunders *et al.*, 2012). Our previous work showed that PiAVR2 promotes the activation of the BR pathway to antagonize immunity (Turnbull *et al.*, 2017). Moreover, as the Solanaceae lack BSU1, PiAVR2 interacts with all three BSL family members (BSL1, BSL2 and BSL3) from potato (*S. tuberosum*). BSL1, BSL2 and BSL3 act as susceptibility (S) factors to enhance *P. infestans* leaf infection; silencing them using virus-induced gene silencing (VIGS) attenuates *P. infestans* infection. BSL1 and BSL3 compromise plant immunity by suppressing elicitor INFESTIN 1 (INF1)-triggered cell death (ICD) (Turnbull *et al.*, 2019).

Rpi-mcq1, an independently evolved NLR protein that is exclusive to South America, also detects PiAVR2. Unlike R2 family members which locate to potato chromosome IV, *Rpi-mcq1* resides on chromosome IX in *S. mochiquense* and only shares c. 30% amino acid identity with R2 (Aguilera-Galvez *et al.*, 2018; Supporting Information Fig. S1). *Phytophthora infestans* infection assays showed that Rpi-mcq1 and the R2 orthologue Rpi-blb3 have an overlapping but distinct resistance to diverse *P. infestans* isolates, and Rpi-blb3 displays a slightly broader disease resistance spectrum compared to Rpi-mcq1 (Aguilera-Galvez *et al.*, 2018).

We aim to address these key questions: Are BSLs required for the recognition of PiAVR2 by these distinct resistance proteins, R2 and Rpi-mcq1? Moreover, as BSLs are phosphatases, are BSL phosphatase activities required for recognition of PiAVR2 by R2 and/or Rpi-mcq1? In this study we demonstrate that, whereas R2 HR exclusively requires BSL1, Rpi-mcq1-triggered immunity is

independent of BSL1, but requires BSL2 and BSL3. Inhibitor treatment assays and expression of phosphatase-dead BSL mutants demonstrated that R2 and Rpi-mcq1 require phosphatase activity to recognize and respond to PiAVR2. Furthermore, whereas coimmunoprecipitation clearly reveals that the formation of a PiAVR2-BSL1-R2 complex is key to R2 HR, we could not demonstrate a direct interaction between PiAVR2-BSL2/BSL3 complexes and Rpi-mcq1. Overall, we conclude that R2 and Rpi-mcq1 detect PiAVR2 via its association with different host target proteins, representing a new R-AVR recognition scenario.

Materials and Methods

Plant material

Nicotiana benthamiana Domin plants were grown under long-day conditions (16 h : 8 h, light : dark photoperiod) at 22°C and 40% humidity. Plants were used for transient expression assays at 4–5 wk old, with 2–3 wk old plants used for VIGS. The top three leaves were infiltrated.

Cloning and constructs

All primers used in this study are listed in Table S1. All constructs with N-terminal tags were generated by Gateway cloning following the manufacturer's instructions (Invitrogen). RFP-PiAVR2 was generated by recombining pDONR201 PiAVR2 into pK7WGR2. Rpi-mcq1 was generated by polymerase chain reaction (PCR) amplification from pKGW Rpi-mcq1 with the primers Rpi-mcq1F1 and Rpi-mcq1R1. GFP-R2, GFP-StBSL1, GFP-StBSL2, GFP-StBSL3, GFP-StBSL1 H468V, GFP-StBSL2 H767V and GFP-StBSL3 H769V were generated by recombination of the entry clone in pDONR201 into pB7WGF2. cMyc-R2, cMyc-Rpi-mcq1, cMyc-StBSL1, cMyc-StBSL2, cMyc-StBSL3, cMyc-StBSL1H468V, cMyc-StBSL2H767V and cMyc-StBSL3H769V were generated by recombination of these same entry clones into pGWB18. PiAVR2-PDEST32, R2-PDEST32 and Rpi-mcq1-PDEST32 were generated by recombination of the entry clones from pDONR201 into PDEST32. StBSL1-PDEST22, StBSL2-PDEST22, StBSL3-PDEST22, R2-PDEST22 and Rpi-mcq1-PDEST22 were generated by recombination of the entry clones from pDONR201 into PDEST22. Site directed mutagenesis was used to introduce point mutations in the active sites of pDONR201 StBSL1, StBSL2 and StBSL3. This was carried out using a Quik-Change II XL kit (Agilent Technologies, Santa Clara, CA, USA) following the manufacturer's instructions. Primer sequences can be found in Table S1.

Agrobacterium-mediated transient gene expression assays

Liquid YEB medium was inoculated with single colonies from plates and incubated with shaking overnight at 28°C. Bacteria were centrifuged at 3900 g for 10 min at room temperature, with the pellet resuspended in agroinfiltration medium (10 mM MES, 10 mM MgCl₂ and 150 mM acetosyringone). The

agroinfiltration medium was kept in the dark for at least 1 h before infiltration. Leaves were infiltrated on the abaxial surface, using a 1 ml syringe after needle wounding.

Hypersensitive response assays

The constructs pB7WGFP2 PiAVR2, pDEST R2 and pKGW Rpi-mcq1 were transferred into the electrocompetent *Agrobacterium* strain GV3101. The combinations of PiAVR2/R2 and PiAVR2/Rpi-mcq1 were co-infiltrated at a final concentration at OD₆₀₀ of 0.3 each, with wild-type (WT) or phosphatase-dead forms of the GFP-StBSLs, or a green fluorescent protein (GFP) empty vector at a final OD₆₀₀ of 0.5 into *N. benthamiana*. For VIGS plants, the different combinations of R proteins and effectors were delivered into *N. benthamiana* leaves 3 wk after initial infiltration with tobacco rattle virus (TRV) constructs. Hypersensitive response was scored at 2–4 d post agroinfiltration from independent experimental replicates, each using three leaves per plant across 7 plants. A leaf sector collapse $\geq 50\%$ was scored as a positive HR, and $< 50\%$ as negative (Fig. S2).

Virus-induced gene silencing

Virus-induced gene silencing constructs consisted of *c.* 250-bp PCR fragments of the gene targeted for silencing. A TRV construct expressing a fragment of GFP was used as a control (Gilroy *et al.*, 2011), and BSL1 and BSL2/3 constructs were as previously described (Saunders *et al.*, 2012; Turnbull *et al.*, 2019). *Agrobacterium* cultures carrying the TRV1 construct were resuspended in agroinfiltration medium at a final concentration at OD₆₀₀ of 0.4, with TRV2 constructs at a final concentration at OD₆₀₀ of 0.5. The two largest leaves of *N. benthamiana* plants at the four-leaf stage were fully syringe-infiltrated with the appropriate *Agrobacterium* mixture. Viral infection was allowed to progress systemically for 3 wk before the plants were used in experiments.

Phosphatase activity assays

Four *N. benthamiana* leaf discs were harvested at 2 d post agroinfiltration. Total protein was extracted in GTEN buffer (10% (v/v) glycerol, 25 mM Tris-HCl (pH 7.5), 1 mM EDTA, and 150 mM NaCl) with 10 mM dithiothreitol, protease inhibitor cocktail, 1 mM phenylmethylsulfonyl fluoride, and 0.2% Nonidet P-40. To immunoprecipitate GFP-BSLs, protein extracts were incubated with GFP-Trap beads (Chromotek, Planegg-Martinsried, Germany) for 1 h at 4°C, followed by centrifugation at 16 200 *g* for 10 min. Beads were washed in 100 μ l PNPP (p-nitrophenyl phosphate) assay buffer (50 mM Tris-HCl, pH 7.0, 0.1 mM CaCl₂), after being washed twice with GTEN buffer. Beads were resuspended in 25 μ l PNPP assay buffer supplemented with 2.8 mM MnCl₂, and pre-incubated for 15 min at 32°C, before adding 30 μ l 5 mg ml⁻¹ PNPP (disodium salt) substrate (5 mg PNPP substrate tablet (11859270; Thermo Scientific, Waltham, MA, USA) in 1 ml 50 mM Tris-HCl, pH 7.0). Activity was monitored over a period of 1 h, with measurements taken at 405 nm using a NanoDrop spectrophotometer. For inhibitor studies, beads were pre-incubated for

1 h at 32°C with inhibitors and a dimethyl sulfoxide (DMSO) control before being resuspended in 25 μ l PNPP assay buffer.

Yeast two-hybrid (Y2H) assays

pDEST32 constructs containing PiAVR2, R2 and Rpi-mcq1 were co-transformed with pDEST22 constructs containing StBSL1, StBSL2, and StBSL3 into the yeast strain MaV203. pDEST32-PiAVR2 was co-transformed with pDEST22-R2 or pDEST22-Rpi-mcq1 into the yeast strain MaV203. pDEST32-PiAVR2, pDEST32-R2 or pDEST32-Rpi-mcq1 was co-transformed with empty pDEST22 as a control. Transformant cells were plated out on media lacking Leu and Trp. Colonies were picked from these plates for the LacZ assay (β -galactosidase activity) using the ProQuest system (Invitrogen), according to the manufacturer's instructions.

Co-immunoprecipitation (co-IP) and immunoblot analysis

For co-IP, *N. benthamiana* leaves were sampled at 4 d post agroinfiltration and immediately frozen in liquid nitrogen. Total protein was extracted in GTEN buffer (10% (v/v) glycerol, 25 mM Tris-HCl (pH 7.5), 1 mM EDTA, and 150 mM NaCl) with 10 mM dithiothreitol, protease inhibitor cocktail, 1 mM phenylmethylsulfonyl fluoride, and 0.2% Nonidet P-40. To immunoprecipitate GFP-tagged or red fluorescent protein (RFP)-tagged proteins, protein extracts were incubated with GFP-Trap or RFP-Trap beads (Chromotek) for 2 h at 4°C, followed by centrifugation at 16 200 *g* for 10 min. Beads were washed three times in GTEN buffer, before resuspending in 2 \times SDS loading buffer. Proteins were separated on 12% Bis-Tris PAGE gels, using an X-blot Mini Cell (Thermo Scientific), followed by transfer to a nitrocellulose membrane (GE Healthcare Life Sciences, Buckinghamshire, UK) using an X10 Blot Module (Thermo Scientific) according to the manufacturer's instructions. Membranes were stained with Ponceau solution to confirm transfer and even loading. Membranes were blocked in 4% milk in 1 \times PBS 0.1% Tween (1 \times PBS-T) with shaking for 1 h at room temperature, before incubation with the appropriate antibodies overnight. Polyclonal GFP antibody (Invitrogen) was used at 1 : 1000, with polyclonal myc- and RFP-antibodies (both SantaCruz Biotechnology, Dallas, TX, USA) used at 1 : 500 and 1 : 4000 respectively. Anti-mouse polyclonal antibody (SantaCruz Biotechnology) was used at 1 : 5000 as a secondary antibody for GFP and myc, with anti-rabbit polyclonal antibody (SantaCruz Biotechnology) used at 1 : 5000 as a secondary antibody for RFP. Protein bands on immunoblots were detected using enhanced chemiluminescence (ECL) substrate (Thermo Scientific) and exposed on Amersham Hyperfilm ECL (GE Healthcare), developed with a Compact X4 Automatic Processor (Xograph Healthcare Ltd, Gloucestershire, UK).

Results

Silencing of different BSL family members shows distinctive effects on R2- and Rpi-mcq1-mediated resistances

To investigate the roles of BSL family members in the recognition of PiAVR2 by R2 and Rpi-mcq1, we performed VIGS in

N. benthamiana to monitor development of the HR. We co-expressed *PiAVR2/R2* or *PiAVR2/Rpi-mcq1* in leaves of plants in which either *NbBSL1* or *NbBSL2* and *NbBSL3* (*BSL2/3*) (Fig. S3) were silenced, using control plants expressing TRV-GFP. *NbBSL1* transcript abundance was reduced in TRV-BSL1 plants but was elevated in TRV:BSL2/3 plants, as observed in Turnbull *et al.* (2019), whereas both *NbBSL2* and *NbBSL3* were reduced in TRV:BSL2/3 plants (Fig. S4a–c). Previously we showed that silencing of *NbBSL2/3* affects BSL1 protein stability but does not reduce transcript level, whereas silencing of *NbBSL1* has no effect on BSL2/3 protein level (Turnbull *et al.*, 2019). As seen previously (Saunders *et al.*, 2012), compared with control TRV-GFP plants, silencing of *BSL1* alone reduced the HR following perception of *PiAVR2* by R2, but did not affect Rpi-mcq1-mediated HR (Rpi-mcq1 HR; Fig. 1). We found that *NbBSL2/3* silencing, using two independent TRV-BSL2/3 constructs, significantly reduced HR triggered by co-expression of R2 and *PiAVR2*, and by co-expression of Rpi-mcq1 and *PiAVR2* (Fig. 1). We confirmed that *PiAVR2*, R2 and Rpi-mcq1 were all stable in plants expressing each of the VIGS constructs (Fig. S4d–f). We further tested HR triggered by another *P. infestans* Avr/potato NLR combination, IPI-O (AVR-blb1)/Rpi-sto1 (Champouret *et al.*, 2009) in *BSL*-silenced plants; no differences in the numbers of HR-forming sites were observed (Fig. 1), indicating that BSLs are specifically required for *PiAVR2*-triggered resistance.

We conclude that the presence of BSL1 is required for the recognition of *PiAVR2* by R2, but not for the recognition of *PiAVR2* by Rpi-mcq1. BSL2 and/or BSL3 are involved in HR triggered by co-expression of *PiAVR2* and R2 or Rpi-mcq1. Because high sequence similarity prevented the independent silencing of *BSL2* and *BSL3* (Turnbull *et al.*, 2019), we were unable to distinguish specific roles of BSL2 or BSL3 in Rpi-mcq1 HR using VIGS.

BSL family members differentially enhance or antagonise Rpi-mcq1- and R2-mediated hypersensitive responses

To further determine whether the BSLs perform distinct roles in the recognition of *PiAVR2* by R2 and Rpi-mcq1, we used transient overexpression in *N. benthamiana*, and scored the HR at 2 to 4 d post-infiltration (dpi). In the leaf panels transiently co-expressing GFP-StBSL1 with *PiAVR2* and R2, we observed a 15% increase in the number of sites forming the HR compared with sites co-infiltrated with the GFP control at 2 dpi (Fig. 2a). By contrast, co-expression of GFP-StBSL2 and GFP-StBSL3, respectively, caused 43% and 34% reductions in the number of *PiAVR2* and R2 infiltration sites forming HR relative to the GFP control at 3 dpi (Fig. 2b,c). Interestingly, the number of inoculation sites forming HR following expression of *PiAVR2* with Rpi-mcq1 was increased in the leaf panels co-expressing GFP-StBSL2 (17%; Fig. 2b) and GFP-StBSL3 (13%; Fig. 2c), whereas Rpi-mcq1 HR was partially attenuated, by 33%, in sites co-expressing GFP-StBSL1 (Fig. 2a). We confirmed that R2, Rpi-mcq1, *PiAVR2* and each of the BSLs were stable when co-expressed (Fig. S5). In conclusion, the three targets of *PiAVR2* – StBSL1, StBSL2 and StBSL3 – are involved in its recognition by R2 or Rpi-mcq1 in distinct ways. Taken with the VIGS result shown in Fig. 1, our results demonstrate that BSL1 is required specifically for the recognition of *PiAVR2* by R2. By contrast, BSL2 and BSL3 are required for *PiAVR2* recognition by Rpi-mcq1.

BSL family members differentially associate with R2 and Rpi-mcq1

StBSL1 is required to mediate R2 recognition of *PiAVR2* (Saunders *et al.*, 2012). Our study confirmed these observations, and further found that StBSL2 and StBSL3 are potentially involved in R2-mediated recognition of *PiAVR2* only indirectly by

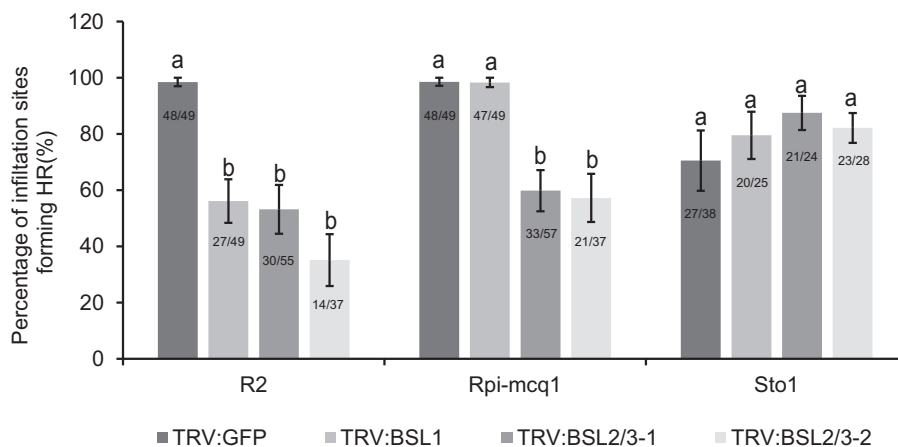


Fig. 1 Rpi-mcq1-mediated hypersensitive response (Rpi-mcq1 HR) requires BSL2/3 but not BSL1 expression. Virus-induced silencing (VIGS) of *NbBSL2/3* in *Nicotiana benthamiana* perturbs both the R2-mediated hypersensitive response (R2 HR) and Rpi-mcq1 HR, while *NbBSL1* silencing specifically compromises R2- HR only. Rpi-Sto1-mediated hypersensitive response shows no significant difference in any silenced plants. The combinations of *PiAVR2* with R2, *PiAVR2* with Rpi-mcq1, or IPIO/AvrBlb1 with Rpi-Sto1, were transiently co-expressed using agroinfiltration. Data shown are the combinations of three independent experimental replicates. Numbers in bars indicate infiltration sites forming HR/total infiltration numbers. Lowercase letters indicate a significant difference compared to TRV:GFP control ($P < 0.001$ in one-way ANOVA, using the Student-Newman-Keuls method). Error bars indicate SEM.

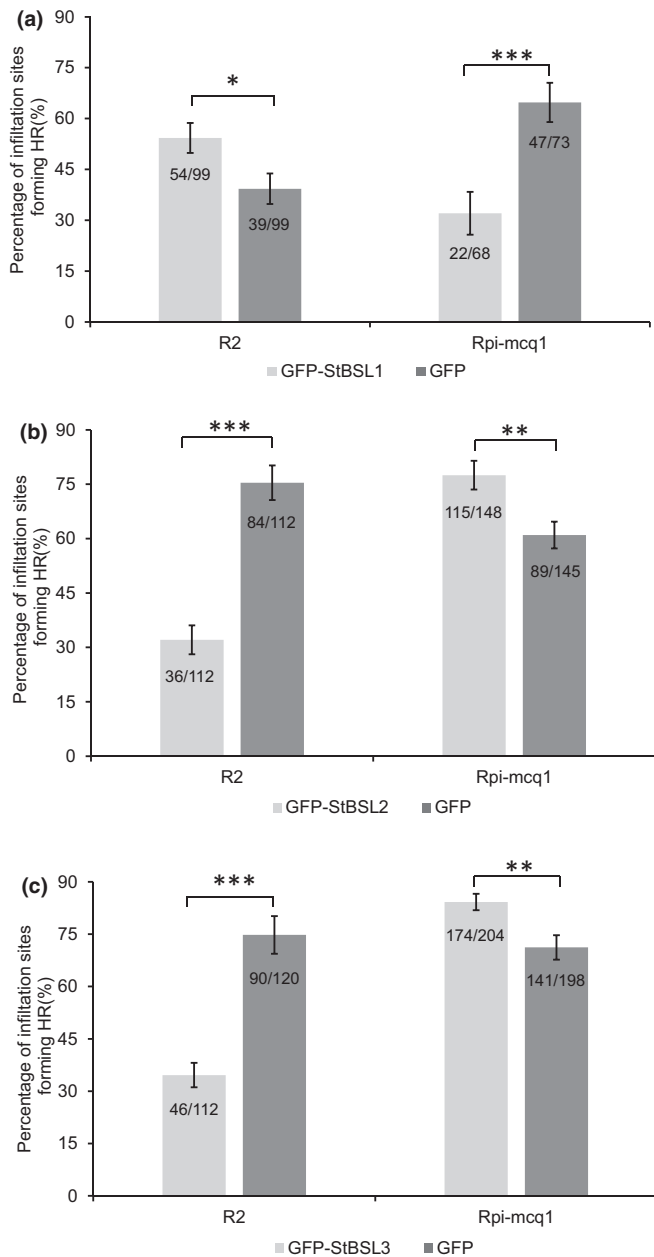


Fig. 2 BSL family members differentially enhance or antagonise the Rpi-mcq1- or R2-mediated hypersensitive response (Rpi-mcq1 HR, R2 HR, respectively). (a) Transient co-expression of GFP-StBSL1 with *PiAVR2*/R2 or *PiAVR2*/Rpi-mcq1 in *Nicotiana benthamiana* shows that GFP-StBSL1 enhances R2 HR (eight independent experimental replicates), whereas GFP-StBSL1 has a suppressive effect on Rpi-mcq1 HR (four independent experimental replicates). (b, c) Transient co-expression of GFP-StBSL2 or GFP-StBSL3 with *PiAVR2*/Rpi-mcq1 indicates that GFP-StBSL2 (seven independent experimental replicates) and GFP-StBSL3 (eight independent experimental replicates) each can enhance Rpi-mcq1 HR in *N. benthamiana*, whereas GFP-StBSL2 and GFP-StBSL3 (five independent experimental replicates each) have a suppressive effect on R2 HR. Numbers in bars indicate infiltration sites forming HR/total infiltration numbers. Statistical analyses were conducted using the *t*-test method. Asterisks indicate significant difference compared to the GFP control (*, $P < 0.05$; **, $P < 0.005$; ***, $P < 0.001$). Error bars indicate SEM.

regulating stability of StBSL1. However, StBSL1 is not required for Rpi-mcq1 HR, whereas StBSL2 and StBSL3 are required for Rpi-mcq1-mediated recognition of *PiAVR2*. Previously, we

demonstrated that there was no direct interaction between R2 and either *PiAVR2* or BSL1 in a Y2H assay (Saunders *et al.*, 2012). Hence, we performed a Y2H assay here to investigate any direct interaction between the BSL proteins and the resistance proteins R2/Rpi-mcq1 and *PiAVR2*. No direct interaction between R2 or Rpi-mcq1 and *PiAVR2* or any BSL protein was detected (Fig. S6). We investigated potential direct and indirect associations of these proteins *in planta* by performing co-IP experiments involving co-expressions of GFP-tagged R2 (GFP-R2) or Rpi-mcq1 (GFP-Rpi-mcq1), RFP-tagged *PiAVR2* protein (RFP-*PiAVR2*), and cMyc-tagged StBSL1 (cMyc-StBSL1), StBSL2 (cMyc-StBSL2) or StBSL3 (cMyc-StBSL3) proteins in different combinations. In line with previous studies (Saunders *et al.*, 2012), cMyc-StBSL1 was pulled down by GFP-R2 only in the presence of RFP-*PiAVR2* (Fig. 3a). Moreover, GFP-R2 was pulled down by RFP-*PiAVR2* only when co-expressed with cMyc-StBSL1 (Fig. S7a). However, we were unable to detect interactions between either cMyc-StBSL2 or cMyc-StBSL3 and GFP-R2, with or without *PiAVR2* (Figs 3a, S7a). Similar results were also obtained when co-expressing GFP-R2 and RFP-*PiAVR2* with tagged *N. benthamiana* orthologues cMyc-NbBSL1, cMyc-NbBSL2 or cMyc-NbBSL3, in that NbBSL1 also exclusively interacted with R2 and only in the presence of *PiAVR2* (Fig. S8a). We found that GFP-Rpi-mcq1 did not associate with RFP-*PiAVR2* directly (Figs 3b, S7b), as was observed previously for GFP-R2 (Saunders *et al.* 2012) (Fig. 3a). In addition, no association between GFP-Rpi-mcq1 and any of the cMyc-StBSLs (Fig. 3b) was observed by co-IP in the absence or presence of RFP-*PiAVR2*. Moreover, whereas RFP-*PiAVR2* co-immunoprecipitated cMyc-StBSL1, cMyc-StBSL2 and cMyc-StBSL3 (Fig. S7b), or cMyc-NbBSL1, cMyc-NbBSL2 and cMyc-NbBSL3 (Fig. S8b) when coexpressed with GFP-Rpi-mcq1, the resistance protein was not also pulled down.

BSL phosphatase activities are required for R2- and Rpi-mcq1-mediated HRs

BSLs are predicted to possess Ser/Thr-protein phosphatase activity, and we therefore investigated whether such activity contributes to the recognition of *PiAVR2* by R2 or Rpi-mcq1. Firstly, the effect of OA, a well-known inhibitor of the Ser/Thr protein phosphatases, was tested to determine whether it inhibits BSL phosphatases. GFP-StBSL constructs were immunoprecipitated following transient expression in *N. benthamiana*, and their activity was measured in the presence or absence of OA *in vitro*. We found that each of the StBSLs possess detectable phosphatase activity: compared with control DMSO treatment, OA decreased phosphatase activity of GFP-StBSL1 by 70% (Fig. 4a), of GFP-StBSL2 by 60% (Fig. 4b) and of GFP-StBSL3 by 49% (Fig. 4c). By contrast, there are no significant differences in BSL phosphatase activities in the presence of bikinin (an inhibitor of the kinase BIN2 downstream of BSLs within the BR signal transduction pathway), or control DMSO (Fig. 4a–c). Elution of GFP-StBSL proteins from GFP-Trap beads and analysis by Western blot revealed that similar protein levels of each BSL were present with each treatment (Fig. S9). In addition, we observed that the

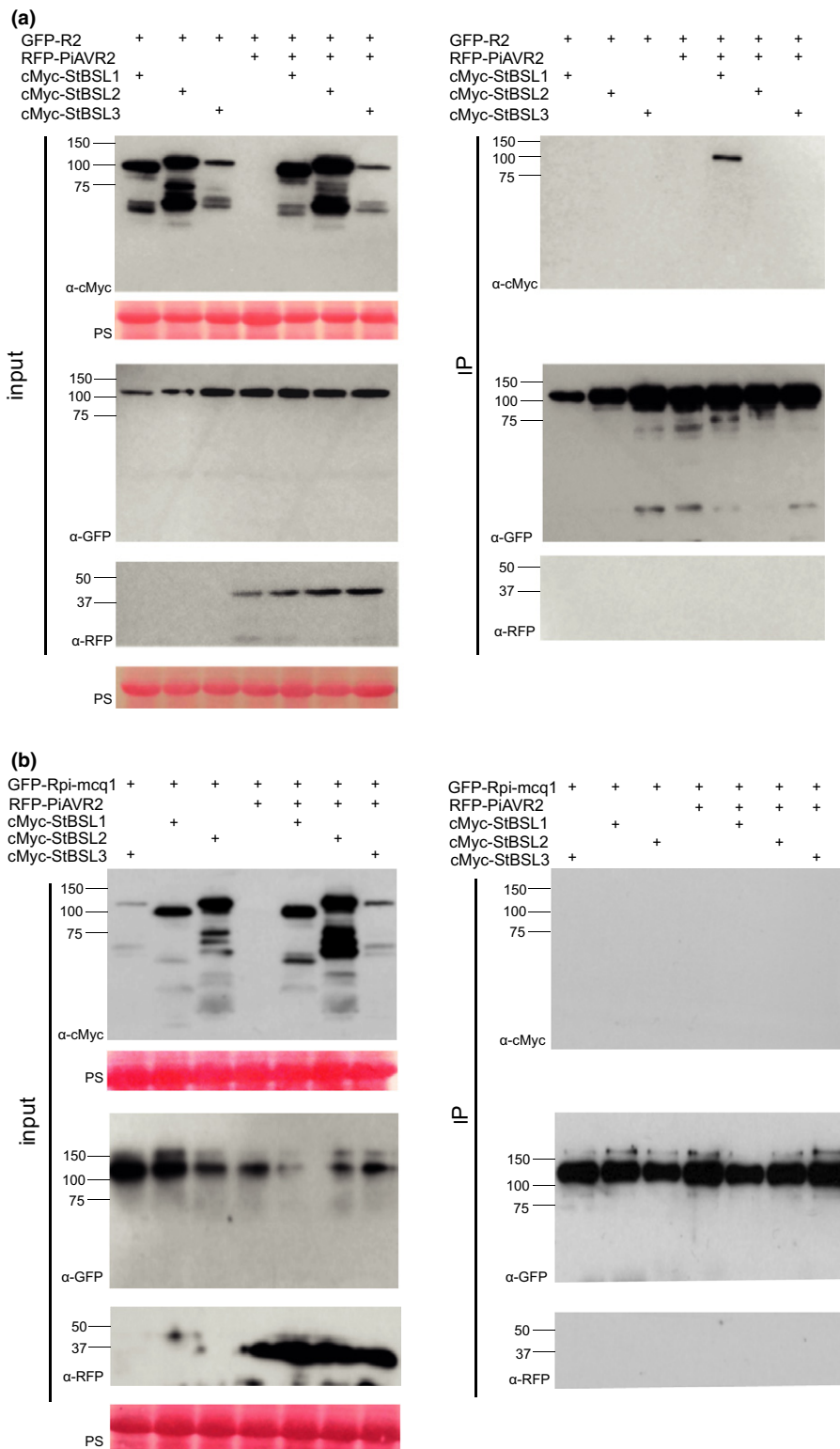


Fig. 3 Conditional interaction of StBSL1 with R2, with no observable interaction between StBSLs and Rpi-mcq1. (a) Immunoprecipitation (IP) of protein extracts from agroinfiltrated *Nicotiana benthamiana* leaves using GFP-Trap beads shows that GFP-R2 associates with cMyc-StBSL1 in the presence of RFP-*PiAVR2*, with no association seen with cMyc-StBSL2 or cMyc-StBSL3. (b) Immunoprecipitation of GFP-Rpi-mcq1 did not reveal any interaction with StBSLs, either in the presence or absence of *PiAVR2*. Expression of constructs in the *N. benthamiana* leaf samples are indicated by the 'plus' symbol (+). Protein size markers are shown in kilodaltons (kDa), and protein loading is indicated by Ponceau stain (PS).

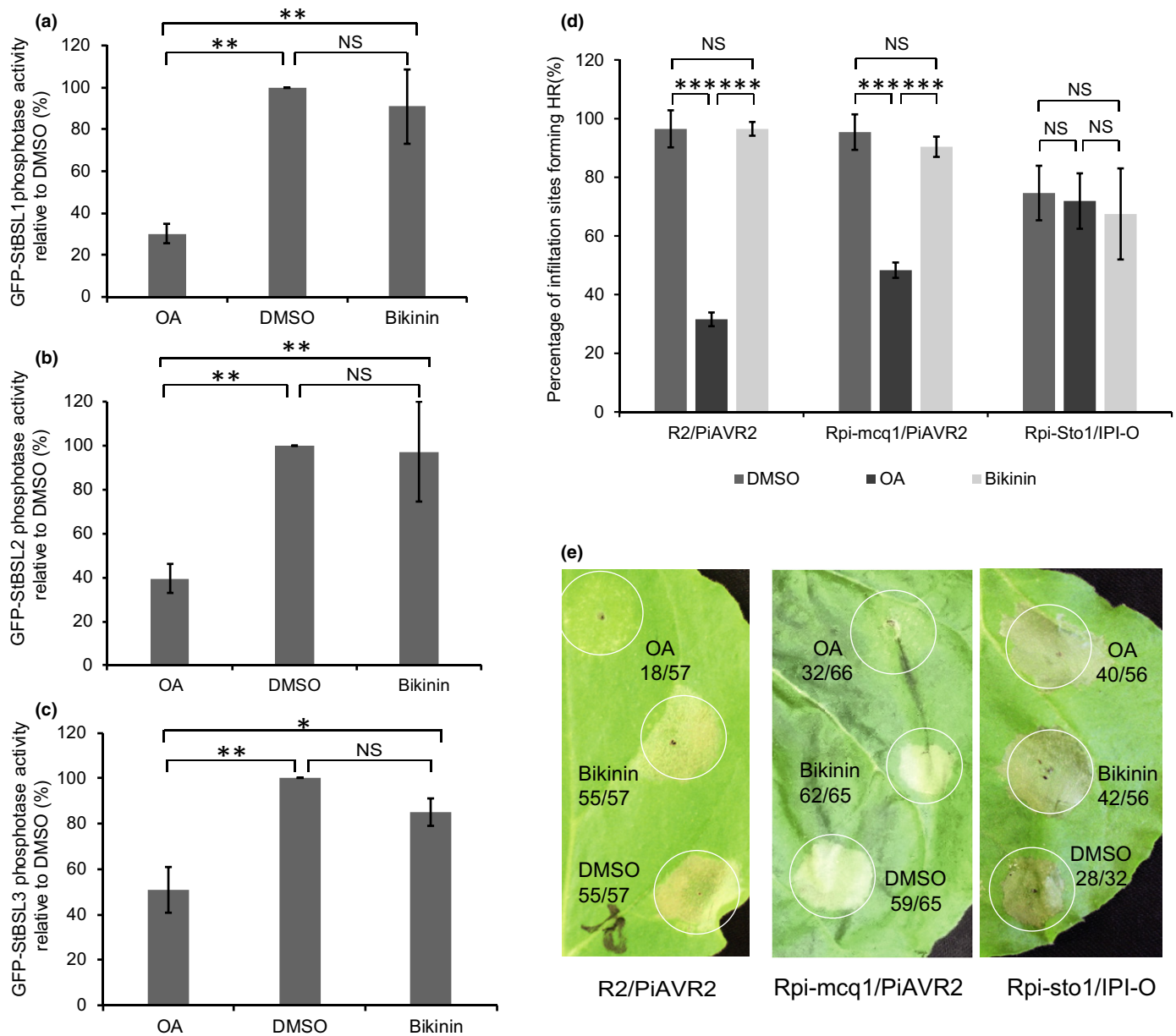


Fig. 4 Phosphatase inhibitor okadaic acid (OA) inhibits BSL activity and suppresses recognition of *PiAVR2* by R2 and Rpi-mcq1. (a–c) GFP-StBSLs were transiently expressed in *Nicotiana benthamiana*. Proteins were immunoprecipitated using GFP beads, and their subsequent phosphatase activity was monitored over a period of 1 h. Significant difference is represented by asterisks (*, $P < 0.05$; **, $P < 0.01$; ns, no significant difference; one-way ANOVA, Student-Newman-Keuls method). Error bars indicate SEM. The results combine data from four independent biological replicates for (a) and (c), and from three independent biological replicates for (b). (d) Agro-infiltration sites co-expressing *PiAVR2*/R2, *PiAVR2*/Rpi-Mcq1 or IPIO/Rpi-sto1 were treated with 62 nM OA, 0.07% dimethyl sulfoxide (DMSO), or 50 μ M bikinin. Okadaic acid was shown to significantly reduce both the R2- and Rpi-mcq1-mediated hypersensitive response (HR), with no effect of DMSO or bikinin. Rpi-sto1-mediated HR was unaffected by OA, bikinin or control DMSO. Results combine data from three independent experimental replicates. Asterisks indicate significant difference compared to the GFP control (***, $P < 0.001$; ns, not significant; one-way ANOVA, using the Student-Newman-Keuls method). Error bars indicate SEM. (e) Typical HR of *N. benthamiana* leaves from (d). White circles indicate the infiltrated area. Numbers next to treatments indicate infiltration sites forming HR/total infiltration numbers.

stability of *PiAVR2*, R2 and Rpi-mcq1 was not detectably altered upon treatment with OA or bikinin (Fig. S10a–c). We tested the effect of OA on the HR triggered by co-expression of R2 or Rpi-mcq1 with *PiAVR2*, as well as Rpi-sto1 with IPI-O. Compared with control DMSO treatment, the *PiAVR2*/R2 HR showed a 65% decrease following treatment with OA, and a 47% reduction in the *PiAVR2*/Rpi-mcq1-induced HR was observed

(Fig. 4d,e). By contrast, no difference was observed in the IPI-O/Rpi-sto1-mediated HR. In comparison, treatment with bikinin allowed all HRs to occur to the same extent as control DMSO treatment (Fig. 4d,e). We did not see any response triggered by treatments with OA, DMSO or bikinin alone (Fig. S10d). The suppression by OA treatment indicates that phosphatase activity is required for the function of these resistance proteins.

Phosphatase-dead StBSLs exert a dominant-negative effect on *PiAVR2*-triggered hypersensitive responses

The Pfam protein family database (Finn *et al.*, 2014) was used to identify the predicted BSL phosphatase active sites, including histidine residue H648 in StBSL1, H769 in StBSL2 and H767 in StBSL3 (Fig. S11a). Phosphatase-dead mutants were generated by site-directed mutagenesis to replace the histidines with valine residues. The activity assay demonstrated that GFP-StBSL1 H648V, GFP-StBSL2 H769V and GFP-StBSL3 H767V phosphatase activities were abolished (Fig. S11b–d). Interestingly, the assay also showed that the phosphatase activity of StBSL3 was considerably lower than that of StBSL1 and StBSL2 (Fig. S10d).

To further determine the importance of the phosphatase activity of StBSL1 in the recognition of R2 by *PiAVR2*, and the significance of phosphatase activities of StBSL2 and StBSL3 in the recognition of Rpi-mcq1 by *PiAVR2*, we co-expressed PD GFP-StBSL1 H648V with *PiAVR2*-R2, and GFP-StBSL2 H769V or GFP-StBSL3 H767V with *PiAVR2*-Rpi-mcq1 in *N. benthamiana* and monitored occurrence of the HR. The data showed that, whereas WT GFP-StBSL1 significantly increased the HR triggered by *PiAVR2* with R2 at 2 dpi, mutant GFP-StBSL1H648V decreased the R2 HR (Fig. 5a). Similarly, whereas WT GFP-StBSL2 and GFP-StBSL3 significantly enhanced the HR triggered by co-expression of *PiAVR2* with Rpi-mcq1, mutant forms GFP-StBSL2 H769V and GFP-StBSL3 H767V significantly attenuated the Rpi-mcq1 HR (Fig. 5b,c) at 3 dpi. Changes in HR are not caused by changes in R2 and Rpi-mcq1 protein stability when co-expressed with PD BSL mutants (Fig. S12). This provides independent evidence supporting the hypothesis that StBSL1 or StBSL2/StBSL3 phosphatase activities are required for recognition of *PiAVR2* by R2 or Rpi-mcq1, respectively.

The Arabidopsis BSLs are known to oligomerise (Kim *et al.*, 2016), leading us to question whether the same occurs with Solanaceae BSLs and whether PD mutant BSLs have an effect on WT BSLs. Co-immunoprecipitation experiments showed a strong interaction between WT and WT forms of each StBSL (Fig. S13). Phosphatase-dead mutants of StBSL1 and StBSL2 retained the ability to interact with their WT counterpart, although these interactions were notably weaker than WT–WT interactions (Fig. S13a,b). The interaction *in planta* of the StBSL3 H767 mutant and WT StBSL3 was undetectable by co-IP (Fig. S13c), which is potentially a consequence of the lower activity or expression of StBSL3 (Fig. S13d). Interestingly, we found that co-expression of cMyc-StBSL mutants with the corresponding WT GFP-StBSL resulted in the reduction of phosphatase activity of WT BSLs when they were immunoprecipitated (Fig. 6). This may explain the reduction of R2 HR following co-expression with StBSL1 H648V, and Rpi-mcq1 HR when co-expressed with StBSL2 H769V or StBSL3 H767V – that is, the mutants exert a dominant negative effect by reducing WT BSL phosphatase activity.

Discussion

We have shown that silencing of *BSL1* results in the reduction of R2 HR (Saunders *et al.* 2012). *PiAVR2* triggers ETI in many wild

Solanum species native to Mexico which possess R2 orthologues clustered on chromosome IV, and also triggers ETI in *S. mochiquense* from Peru, which carries the unrelated NLR-encoding gene *Rpi-mcq1* on chromosome IX (Aguilera-Galvez *et al.*, 2018; Aguilera-Galvez *et al.*, 2020). Our objectives were to understand whether the two evolutionarily distinct NLR classes detect *PiAVR2* via the same effector targets, the BSLs, and whether BSL family members perform similar roles in R2 and Rpi-mcq1 HR. Intriguingly, a difference was immediately apparent: whilst R2 HR was reduced in plants with either *BSL1* or combined *BSL2/BSL3* silencing, Rpi-mcq1 HR was reduced only in *BSL2/BSL3* silenced plants, with no effect of *BSL1* silencing (Fig. 1). Notably, *BSL2/BSL3* silencing results in a BSL-null plant, as – despite *BSL1* transcript levels being unaffected – the protein itself becomes undetectable (Turnbull *et al.*, 2019). This perhaps indicates that *BSL1* requires the action of *BSL2* and/or *BSL3* for stability. By contrast, whereas *BSL2* and *BSL3* are undetectable at the transcript or protein levels in *BSL2/3*-silenced plants, their transcripts and proteins are readily detectable in *BSL1*-silenced plants (Turnbull *et al.*, 2019). Thus R2 HR requires *BSL1*, whereas Rpi-mcq1 requires *BSL2* and/or *BSL3* and does not require *BSL1*.

To clarify and complement the silencing results, cell death assays with co-expressed *PiAVR2*, R2/Rpi-mcq1, and either *BSL1*, *BSL2* or *BSL3* showed clear opposing effects of the BSL family members on R2 and Rpi-mcq1 activity. *BSL1* enhanced the R2 HR whilst suppressing that of Rpi-mcq1, whereas *BSL2* or *BSL3* achieved the opposite – suppressing the R2 HR, whilst enhancing that of Rpi-mcq1 (Fig. 2). Taken together with the silencing results, these data show that recognition of *PiAVR2* by R2 is dependent on *BSL1*, whereas recognition of *PiAVR2* by Rpi-mcq1 is reliant on *BSL2* and/or *BSL3*.

Co-immunoprecipitation assays indicated that R2 monitors the interaction of *PiAVR2* with *BSL1* specifically, and that *PiAVR2* interacts with R2 only when co-expressed with *BSL1*, suggesting that the three proteins are present together in a stable complex. By contrast, there was no detectable interaction of Rpi-mcq1 with any of the BSL family members, either in the presence or absence of *PiAVR2* (Figs 3, S7, S8). This information points to a model in which potato StBSL1 directly and exclusively facilitates effector recognition by R2, whereas a weak and transient interaction between Rpi-mcq1 and *BSL2/3*, or an intermediary protein (or a number of proteins) in addition to StBSL2 and/or StBSL3, may be required to facilitate effector recognition by Rpi-mcq1 (Fig. 7a).

What is common to both R2 and Rpi-mcq1 HR is the requirement for phosphatase activity, with the inhibitor OA exerting a strong suppressive effect (Fig. 4). Notably, OA inhibits phosphatase activity of all three BSLs *in vitro* (Fig. 4), prompting the hypothesis that phosphatase activity of the BSLs themselves may be a driving factor in transducing *PiAVR2* recognition into R2/Rpi-mcq1 activation (Fig. 7). To investigate this further, PD versions of the BSLs were generated and were shown to lack the ability of the WT forms to enhance R2/Rpi-mcq1-dependent HR. Moreover, *BSL1*-PD reduced the levels of R2 HR, and *BSL2*-PD or *BSL3*-PD reduced the levels of Rpi-mcq1 HR (Fig. 5). The

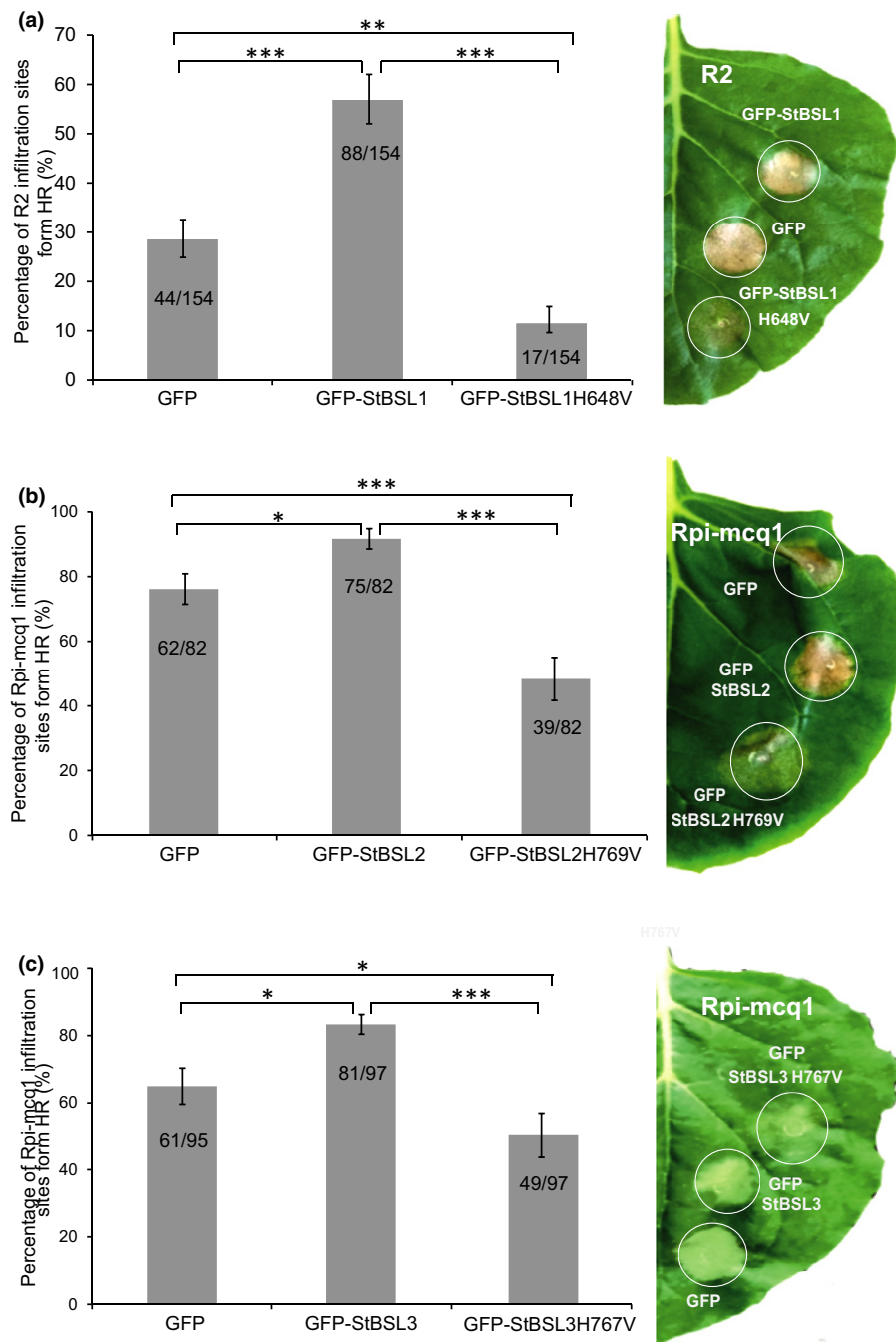


Fig. 5 Phosphatase-dead BSLs exert a dominant-negative effect on *PiAVR2*-triggered hypersensitive responses (HRs). (a) Transient co-expression of GFP-StBSL1, GFP-StBSL1 H648V, or GFP with *PiAVR2*/R2 in *Nicotiana benthamiana* shows that, whereas wild-type (WT) StBSL1 accelerates R2-mediated hypersensitive response (HR), StBSL1 H648V has a suppressive effect compared to the GFP control. The results combine data from six independent experimental replicates. (b) Transient co-expression of GFP-StBSL2, GFP-StBSL2 H769V, or GFP with *PiAVR2*/Rpi-mcq1 in *N. benthamiana* indicates that WT StBSL2 accelerates the Rpi-mcq1-mediated HR (Rpi-mcq1 HR), with GFP-StBSL2 H769V having a suppressive effect compared to the GFP control. Results combine data from five independent experimental replicates. (c) Transient co-expression of GFP-StBSL3, GFP-StBSL3 H767V or GFP with *PiAVR2*/Rpi-mcq1 in *N. benthamiana* indicates that WT StBSL3 accelerates the Rpi-mcq1 HR, with GFP-StBSL3 H767V having a suppressive effect compared to the GFP control. The results combine data from five independent experimental replicates. Numbers in bars indicate infiltration sites forming HR/total infiltration numbers. An example leaf is shown to the right of each graph. Asterisks indicate significant difference (*, $P < 0.05$; **, $P < 0.005$; ***, $P < 0.001$; one-way ANOVA, Student-Newman-Keuls method). Square brackets linking the bars indicate the data that are being compared. Error bars indicate SEM.

dominant-negative effect of the PD mutants on WT forms was also observed *in vitro* when phosphatase activity of all three WT BSLs was significantly reduced by co-expression of the mutant

form (Fig. 6). Wild-type-phosphatase-dead interaction, albeit at a lower level than WT-WT interaction, was confirmed for StBSL1 and StBSL2 (Fig. S13). Whilst we were unable to detect

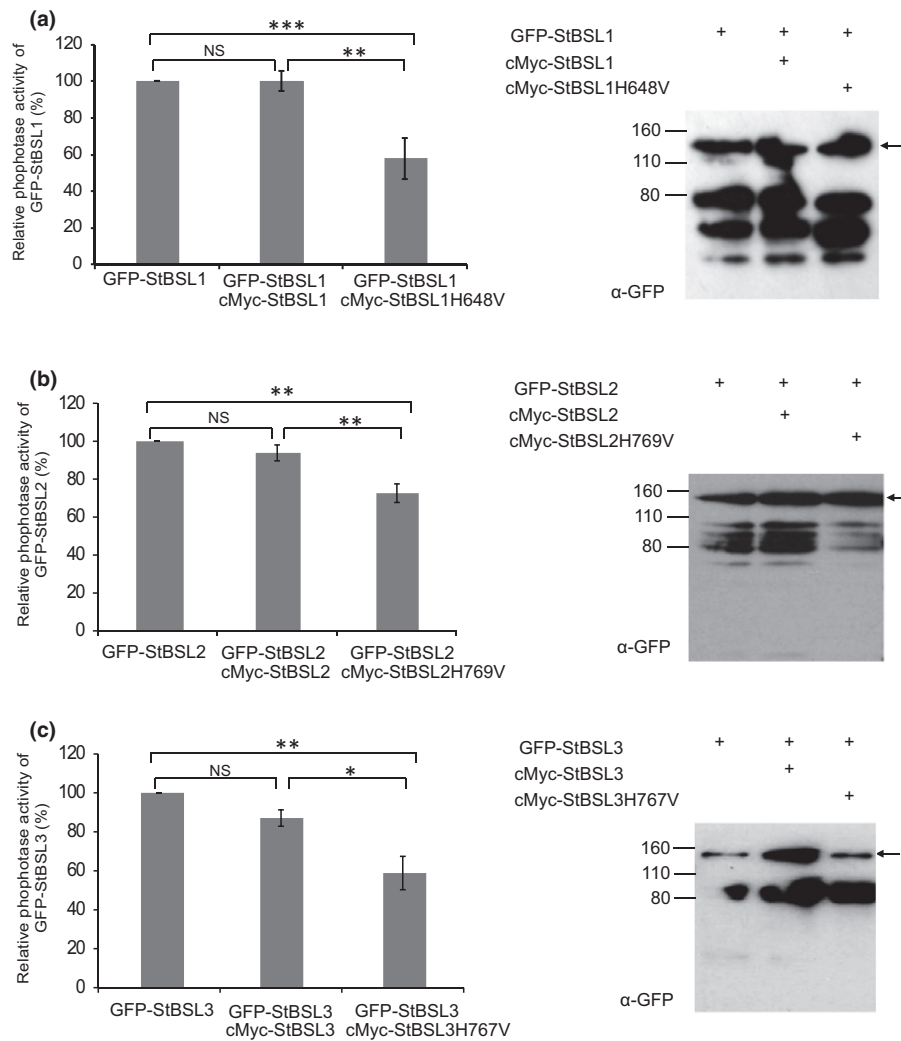


Fig. 6 Co-expression of phosphatase-dead StBSLs suppresses phosphatase activity of the wild-type (WT) forms. (a–c) Green fluorescent protein (GFP)-tagged WT, and cMyc-tagged mutant forms of the StBSLs were co-expressed in *Nicotiana benthamiana*, with leaf material harvested 2 d post-infiltration (dpi) for immunoprecipitation using GFP-Trap beads. In the presence of the mutant form, WT forms of all three family members show a significant reduction of phosphatase activity. Results combine data from six independent experimental replicates for (a), and three independent experimental replicates for (b) and (c). Asterisks indicate significant difference (*, $P < 0.05$; **, $P < 0.005$; ***, $P < 0.001$; ns, not significant; one-way ANOVA, Student–Newman–Keuls method). Square brackets linking the bars indicate the data that are being compared. Error bars indicate SEM. After the activity assay, WT GFP-BSL proteins were eluted from the beads and analysed by immunoblots (to the right of corresponding activity graphs) to confirm stability. Protein size markers are indicated in kilodaltons (kDa). Arrows indicate the GFP-BSL WT fusion proteins. The ‘plus’ symbol (+) indicates construct expression.

WT–PD interaction for StBSL3, the observation that StBSL3-PD reduces phosphatase activity of the WT when co-expressed raises the possibility that these do indeed retain some interaction that is below the detection limit of our co-IP experiments.

R2 and Rpi-mcq1 may themselves be substrates for dephosphorylation by the BSLs, or they may interact with other host proteins that are substrates – ‘adaptor’ proteins that in turn lead to activation of the resistance proteins. In addition, phosphatase activity of BSLs may be required for the formation of a protein complex including *Pi*AVR2-adaptors R2/Rpi-mcq1; or, alternatively, dephosphorylated *Pi*AVR2 may be essential for recognition by the resistance proteins. In the Arabidopsis BR pathway, the BSL family members are interacting partners of the brassinosteroid signalling kinases (BSKs) and act to transduce BR perception from the activated BRI1 receptor to the kinase BIN2. BIN2

is inactivated by BSU1-mediated dephosphorylation, enabling the rapid dephosphorylation of its substrates, the transcription factors BZR1 and BZR2, by PP2A (Mora-Garcia *et al.*, 2004; Kim *et al.*, 2009; Maselli *et al.*, 2014). The inhibitor bikinin, which inhibits BIN2 kinase activity (representing an outcome of BSL activity), did not accelerate R2 or Rpi-mcq1 CD (Fig. 4), unlike overexpression of the BSL phosphatases themselves (Figs 2, 5). This excludes BIN2 of the BR pathway as an intermediary substrate. Future searches for other BSL-interacting proteins, and analyses of phosphosites present on the NLR proteins themselves, are needed to reveal the precise mechanism by which R2 and Rpi-mcq1 are activated, and the roles of phosphorylation in that (Fig. 7a).

Effector recognition by a plant NLR may be direct, or indirect by means of an intermediate host target. In some cases, this may

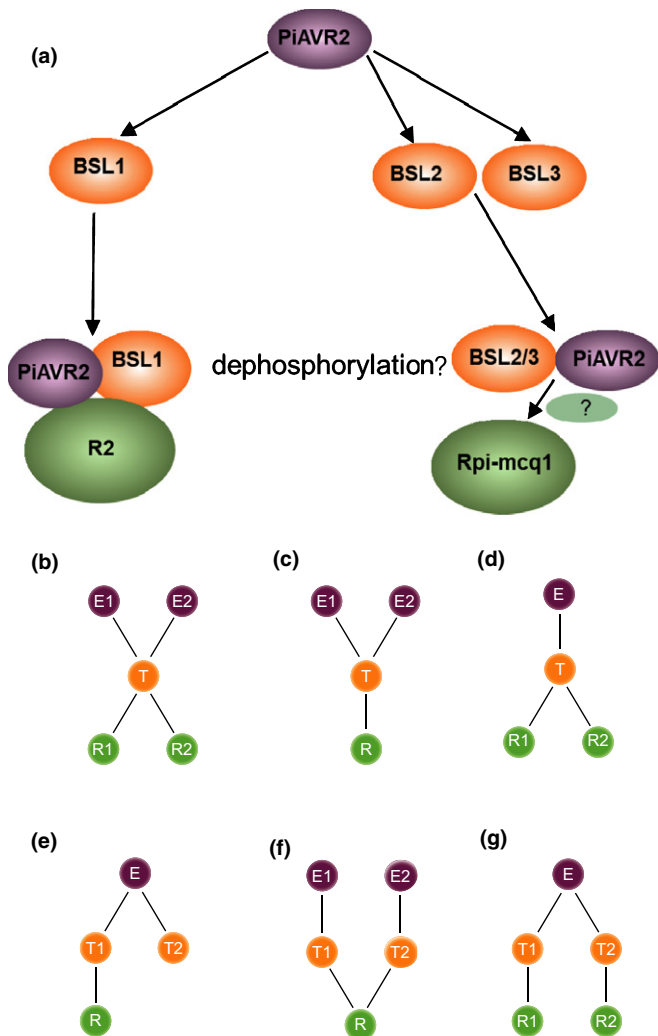


Fig. 7 Model depicting the proposed interaction between BSL family members and R2/Rpi-mcq1 in the recognition of *PiAVR2*. (a) The *Phytophthora infestans* effector *PiAVR2* can interact with all three members (BSL1, BSL2 and BSL3) of the BSL family in potato and *Nicotiana benthamiana*. R2 monitors the interaction of *PiAVR2* with BSL1, resulting in the formation of a complex and subsequent immune activation and hypersensitive response (HR). By contrast, Rpi-mcq1 requires the interaction of *PiAVR2* with BSL2 and/or BSL3 and does not appear to form a detectable complex, perhaps implicating intermediary proteins (in light green) involved in the recognition and immune response. (b–g) A number of scenarios have been described by which effector (E) recognition by a Nucleotide binding leucine-rich repeat (NLR; denoted 'R' in the figure) is mediated by an intermediated target/interactor (T). In scenario (b), multiple effectors converge on the same target, with activities monitored by independent NLRs. In scenario (c), multiple effectors can interact with the same target, with both being recognised by the same NLR. In scenario (d), independently evolved NLRs can recognise the same effector–target interaction. In scenario (e), an effector may interact with multiple targets, with only one of these being monitored by an NLR. In scenario (f), the interaction of multiple effectors with independent targets can be monitored by the same NLR. Finally, in (g), a single effector (*PiAVR2*) may have multiple targets (BSL1 vs BSL2/3), which are monitored by independent NLRs (R2 and Rpi-mcq1).

be a straightforward case of one effector/one target/one resistance protein. Yet complexity beyond this model does exist (Fig. 7b–f), and this additional complexity is likely to be revealed in time. A

number of scenarios have been reported by which R-AVR recognition is mediated by the effector target. In a first scenario, a specific target of independently evolved effectors can mediate recognition by independently evolved NLRs (Fig. 7b). A classic example is RIN4, a target of *AvrRpm1* and *AvrRpt2*, each of which is recognized, respectively, by cognate NLRs RPM1 and RPS2 (Mackey *et al.*, 2002). Whereas RPM1 monitors *AvrRPM1*-mediated change in the phosphorylation status of RIN4, RPS2 monitors *AvrRpt2*-mediated proteolysis of RIN4 (Kim *et al.*, 2005). A second scenario reveals that independently evolved effectors can be recognized by a single NLR that monitors a key change that they make to their shared target (Fig. 7c). Thus, RPM1 can detect a change in the phosphorylation of RIN4 that is mediated by both *AvrRPM1* and *AvrB* (Chung *et al.*, 2011). A third scenario demonstrates that the actions of a specific effector upon its target can be monitored by independently evolved NLRs (Fig. 7d). The targeting of RIN4 by *AvrB* can be detected not only by RPM1 from *Arabidopsis*, but also by the independently evolved NLR Rpg1-b from soybean (Ashfield *et al.*, 2004; Selote & Kachroo, 2010). More recently, it has been shown that proteolytic cleavage of RIN4 by *AvrRpt2* is detected by RPS2 from *Arabidopsis* and the unrelated NLR MR5 from apple (Prokhorchik *et al.*, 2020). A fourth scenario reveals that an effector with multiple targets can be detected by an NLR that monitors just one of them (Fig. 7e). That is the case for the *Magnaporthe oryzae* effector *AvrPiz-t*, which targets two RING E3 ubiquitin ligases APIP6 and APIP10 (Park *et al.*, 2012, 2016), the bZIP transcription factor APIP5 (Wang *et al.*, 2016), a nucleoporin-like protein APIP12 (Tang *et al.*, 2017), and a potassium channel protein AKT1 (Shi *et al.*, 2018). The NLR receptor *Piz-t* only monitors one of these targets, APIP10, to detect *AvrPiz-t* (Park *et al.*, 2016). In a fifth scenario, multiple effectors with independent targets can be recognised by the same NLR (Fig. 7f). This is the case for the *Arabidopsis* NLR ZAR1, which indirectly recognizes effectors HopZ1a and HopF2 from *Pseudomonas syringae*, and *AvrAC* from *Xanthomonas campestris*, by associating with RLCK family XII pseudokinases ZED1, ZRK3 and ZRK1/RKS1, respectively (Lewis *et al.*, 2010; Lewis *et al.*, 2013; Wang *et al.*, 2015; Seto *et al.*, 2017). ZED1 has been proposed as a decoy substrate monitored by ZAR1 to detect acetylation of other (kinase) substrates of HopZ1a (Lewis *et al.*, 2013, 2014; Roux *et al.*, 2014; Bastedo *et al.*, 2019). By contrast, ZRK1/RKS1 functions as an adaptor for ZAR1 by recruiting PBL2 proteins that are uridylylated by *AvrAC* (Wang, *et al.*, 2015, 2019a,b). However, no study to date appears to describe a pathogen effector monitored by two independent resistance proteins, each guarding distinct but related paralogous targets.

We have shown that two evolutionarily unrelated R proteins, R2 and Rpi-mcq1 (Aguilera-Galvez *et al.*, 2018), monitor the activity of the *P. infestans* effector *PiAVR2* on different host targets, respectively the kelch-repeat phosphatases BSL1 and BSL2/BSL3. Both recognition events require phosphatase activity of the corresponding BSLs, with BSL1 playing a crucial role in the recognition of *PiAVR2* by R2, and BSL2 and BSL3 required for the recognition of *PiAVR2* by Rpi-mcq1 (Fig. 7a). To our knowledge, this represents a novel case of convergent evolution –

an example of a pathogen effector recognised by two independent NLR proteins by means of distinct host protein targets (Fig. 7g). ‘Double recognition’ of an effector, via two distinct targets and NLRs, presents an intriguing opportunity for the development of more durable disease resistance strategies in the future. Stacking different NLRs that can detect the same effector through distinct mechanisms can buttress against defeat of one R protein mechanism through simple structure/function mutations in an effector. For example, mutations in *PiAVR2* that prevent interaction with BSL1 and thus escape R2 recognition would still be detected by Rpi-Mcq1. Such stacks may be useful where the virulence function of an effector is robust because it interacts with multiple paralogous targets that are redundant for susceptibility function. Functionally distinct *R* genes should be prioritised for resistance breeding over *R* genes that have similar mechanisms.












Acknowledgements

We are thankful for financial support from the Biotechnology and Biological Sciences Research Council (BBSRC) grants BB/P020569/1, BB/N009967/1 and BB/L026880/1, ERC-Advanced grant PathEvoMe (787764), the Scottish Government Rural and Environment Science and Analytical Services Division (RESAS) and the National Natural Science Foundation of China (31761143007).

Author contributions

PRJB, HXW, VV and EG planned and designed the research. HXW, FT, DT, CA-G, SB and SN performed experiments and analysed data. PRJB, HXW, JDGJ, IH, ZDT and VV wrote the manuscript with input from all authors.

ORCID

Paul R. J. Birch  <https://orcid.org/0000-0002-6559-3746>
 Susan Breen  <https://orcid.org/0000-0001-5232-9973>
 Eleanor Gilroy  <https://orcid.org/0000-0002-5301-4268>
 Ingo Hein  <https://orcid.org/0000-0002-0128-2084>
 Jonathan D. G. Jones  <https://orcid.org/0000-0002-4953-261X>
 Shaista Naqvi  <https://orcid.org/0000-0001-7972-7381>
 Zhendong Tian  <https://orcid.org/0000-0002-3271-5372>
 Franziska Trusch  <https://orcid.org/0000-0003-0608-202X>
 Dionne Turnbull  <https://orcid.org/0000-0002-4831-8064>
 Vivianne Vleeshouwers  <https://orcid.org/0000-0002-8160-4556>
 Haixia Wang  <https://orcid.org/0000-0001-5709-4018>

References

- Aguilera-Galvez C, Champouret N, Rietman H, Lin X, Wouters D, Chu Z, Jones J, Vossen Jh, Visser R, Wolters PJ *et al.* 2018. Two different *R* gene loci co-evolved with *Avr2* of *Phytophthora infestans* and confer distinct resistance specificities in potato. *Studies in Mycology* 89: 105–115.
- Aguilera-Galvez C, Chu Z, Omy SH, Wouters D, Gilroy EM, Vossen VJH, Visser RGF, Birch PRJ, Jones JDG, Vleeshouwers VGAA. 2020. The *Rpi-mcq1* resistance gene family recognizes *Avr2* of *Phytophthora infestans* but is distinct from *R2*. *BioRxiv*. doi: 10.1101/2020.10.08.331181.
- Ashfield T, Ong LE, Nobuta K, Schneider CM, Innes RW. 2004. Convergent evolution of disease resistance gene specificity in two flowering plant families. *Plant Cell* 16: 309–318.
- Bastedo DP, Khan M, Martel A, Seto D, Kireeva I, Zhang J, Masud W, Millar D, Lee JY, Lee A-Y *et al.* 2019. Perturbations of the ZED1 pseudokinase activate plant immunity. *PLoS Pathogens* 15: e1007900.
- Birch PRJ, Bryan G, Fenton B, Gilroy EM, Hein I, Jones J, Taylor M, Torrance L, Toth IK. 2012. Crops that feed the world. Potato: are the trends of increased global production sustainable? *Food Security* 4: 477–508.
- Champouret N. 2010. *Functional genomics of Phytophthora infestans effectors and solanum resistance genes*. PhD dissertation, Wageningen, the Netherlands: Wageningen University.
- Champouret N, Bouwmeester K, Rietman H, van der Lee T, Maliepaard C, Heupink A, van de Vondervoort PJ, Jacobsen E, Visser RG, van der Vossen EA *et al.* 2009. *Phytophthora infestans* isolates lacking class I ipiO variants are virulent on Rpi-blb1 potato. *Molecular Plant–Microbe Interactions* 22: 1535–1545.
- Chen X, Lewandowska D, Armstrong MR, Baker K, Lim TY, Bayer M, Harrower B, McLean K, Jupe F, Witek K *et al.* 2018. Identification and rapid mapping of a gene conferring broad-spectrum late blight resistance in the diploid potato species *Solanum verrucosum* through DNA capture technologies. *Theoretical and Applied Genetics* 131: 1287–1297.
- Chung EH, da Cunha L, Wu AJ, Gao Z, Cherkis K, Afzal AJ, Mackey D, Dangl JL. 2011. Specific threonine phosphorylation of a host target by two unrelated type III effectors activates a host innate immune receptor in plants. *Cell Host & Microbe* 9: 125–136.
- Eitas TK, Dangl JL. 2010. NB-LRR proteins: pairs, pieces, perception, partners, and pathways. *Current Opinion in Plant Biology* 13: 472–477.
- Elmore JM, Lin ZJ, Coaker G. 2011. Plant NB-LRR signaling: upstreams and downstreams. *Current Opinion in Plant Biology* 14: 365–371.
- Finn RD, Miller BL, Clements J, Bateman A. 2014. iPFam: a database of protein family and domain interactions found in the Protein Data Bank. *Nucleic Acids Research* 42(Database issue): D364–D373.
- Foster SJ, Park TH, Pel M, Brigneti G, Sliwka J, Jagger L, van der Vossen E, Jones JDG. 2009. *Rpi-vnt1.1*, a *Tm-2(2)* homolog from *Solanum venturii*, confers resistance to potato late blight. *Molecular Plant–Microbe Interactions* 22: 589–600.
- Gilroy EM, Breen S, Whisson SC, Squires J, Hein I, Kaczmarek M, Turnbull D, Boevink PC, Lokossou A, Cano LM *et al.* 2011. Presence/absence, differential expression and sequence polymorphisms between *PiAVR2* and *PiAVR2*-like in *Phytophthora infestans* determine virulence on *R2* plants. *New Phytologist* 191: 763–776.
- Hayward AC. 1991. Bacterial wilt caused by *Pseudomonas solanacearum*. *Annual Review of Phytopathology* 29: 65–87.
- Hein I, Birch PRJ, Danan S, Lefebvre V, Acheng O, Damaris G, Christiane T, Friederike B, Glenn J. 2009. Progress in mapping and cloning qualitative and quantitative resistance against *Phytophthora infestans* in potato and its wild relatives. *Potato Research* 52: 215–227.
- Jo KR, Visser RGF, Jacobsen E, Vossen JH. 2015. Characterisation of the late blight resistance in potato differential MaR9 reveals a qualitative resistance gene, *R9a*, residing in a cluster of Tm-22 homologs on chromosome IX. *Theoretical and Applied Genetics*. 128: 931–941.
- Jones JDG, Dangl JL. 2006. The plant immune system. *Nature* 444: 323–329.
- Jones JDG, Foster SJ, Chu ZH, Park TH, Van Der Vossen EAG, Pel MA, Visser RGF. 2007. *Late blight resistance genes and methods*. US patent W0 2009013468 A2.
- Jones JDG, Vance RE, Dangl JL. 2016. Intracellular innate immune surveillance devices in plants and animals. *Science* 354: aaf6395.
- Jones JDG, Witek K, Verweij W, Jupe F, Cooke D, Dorling S, Tomlinson L, Smoker M, Perkins S, Foster S. 2014. Elevating crop disease resistance with cloned genes. *Philosophical Transactions of the Royal Society of London. Series B: Biological Sciences* 369: 20130087.
- Khan M, Subramaniam R, Desveaux D. 2016. Of guards, decoys, baits and traps: pathogen perception in plants by type III effector sensors. *Current Opinion in Microbiology* 29: 49–55.

- Kim EJ, Youn JH, Park CH, Kim TW, Guan S, Xu S, Burlingame AL, Kim YP, Kim SK, Wang ZY *et al.* 2016. Oligomerization between BSU1 family members potentiates brassinosteroid signaling in *Arabidopsis*. *Molecular Plant* 9: 178–181.
- Kim MG, da Cunha L, McFall AJ, Belkhadir Y, DebRoy S, Dangi JL, Mackey D. 2005. Two *Pseudomonas syringae* type III effectors inhibit RIN4-regulated basal defense in *Arabidopsis*. *Cell* 121: 749–759.
- Kim TW, Guan S, Sun Y, Deng Z, Tang W, Shang JX, Sun Y, Burlingame AL, Wang ZY. 2009. Brassinosteroid signal transduction from cell-surface receptor kinases to nuclear transcription factors. *Nature Cell Biology* 11: 1254–1260.
- Kuhl JC, Hanneman REJ, Havey MJ. 2001. Characterization and mapping of Rpi1, a late blight resistance locus from diploid (1EBN) Mexican *Solanum pinnatisectum*. *Molecular Genetics and Genomics* 65: 977–985.
- Lewis JD, Lee AH, Hassan JA, Wan J, Hurley B, Jhingree JR, Wang PW, Lo T, Youn JY, Guttman DS *et al.* 2013. The *Arabidopsis* ZED1 pseudokinase is required for ZAR1-mediated immunity induced by the *Pseudomonas syringae* type III effector HopZ1a. *Proceedings of the National Academy of Sciences, USA* 110: 18722–18727.
- Lewis JD, Lo T, Bastedo P, Guttman DS, Desveaux D. 2014. The rise of the undead: pseudokinases as mediators of effector-triggered immunity. *Plant Signaling and Behavior* 9: e27563.
- Lewis JD, Wu R, Guttman DS, Desveaux D. 2010. Allele-specific virulence attenuation of the *Pseudomonas syringae* HopZ1a type III effector via the *Arabidopsis* ZAR1 resistance protein. *PLoS Genetics* 6: 1–13.
- Li X, Van Eck HJ, Rouppe van der Voort JNAM, Huigen DJ, Stam P, Jacobsen E. 1998. Autotetraploids and genetic mapping using common AFLP markers: The R2 allele conferring resistance to *Phytophthora infestans* mapped on potato chromosome 4. *TAG. Theoretical and Applied Genetics* 96: 1121–1128.
- Liu T, Yu Y, Cai X, Tu W, Xie C, Liu J. 2016. Introgression of bacterial wilt resistance from *Solanum melongena* to *S. tuberosum* through asymmetric protoplast fusion. *Plant Cell, Tissue and Organ Culture* 125: 433–443.
- Lokossou AA, Park TH, van Arkel G, Arens M, Ruyter-Spira C, Morales J, Whisson SC, Birch PR, Visser RG, Jacobsen E *et al.* 2009. Exploiting knowledge of R/Avr genes to rapidly clone a new LZ-NBS-LRR family of late blight resistance genes from potato linkage group IV. *Molecular Plant–Microbe Interactions* 22: 630–641.
- Mackey D, Holt BF, Wiig A, Dangi JL. 2002. RIN4 interacts with *Pseudomonas syringae* type III effector molecules and is required for RPM1-mediated resistance in *Arabidopsis*. *Cell* 108: 743–754.
- Maselli GA, Slamovits CH, Bianchi JI, Vilarraza-Blasi J, Caño-Delgado AI, Mora-García S. 2014. Revisiting the evolutionary history and roles of protein phosphatases with Kelch-like domains in plants. *Plant Physiology* 164: 1527–1541.
- Mora-García S, Vert G, Yin Y, Cano-Delgado A, Cheong H, Chory J. 2004. Nuclear protein phosphatases with Kelch-repeat domains modulate the response to brassinosteroids in *Arabidopsis*. *Genes & Development* 18: 448–460.
- Park CH, Chen S, Shirsekar G, Zhou B, Khang CH, Songkumarn P, Afzal AJ, Ning Y, Wang R, Bellizzi M *et al.* 2012. The *Magnaporthe oryzae* effector AvrPiz-t targets the RING E3 ubiquitin ligase APIP6 to suppress pathogen-associated molecular pattern-triggered immunity in rice. *Plant Cell* 24: 4748–4762.
- Park CH, Shirsekar G, Bellizzi M, Chen S, Songkumarn P, Xie X, Shi X, Ning Y, Zhou B, Suttiviriya P *et al.* 2016. The E3 ligase APIP10 connects the effector AvrPiz-t to the NLR receptor Piz-t in rice. *PLoS Pathogens* 12: e1005529.
- Park TH, Foster S, Brigneti G, Jones JDG. 2009. Two distinct potato late blight resistance genes from *Solanum berthaultii* are located on chromosome 10. *Euphytica* 165: 269–278.
- Park TH, Gros J, Sikkema A, Vleeshouwers VGAA, Muskens M, Allefs S, Jacobsen E, Visser RGF, van der Vossen EAG. 2005a. The late blight resistance locus *Rpi-blb3* from *Solanum bulbocastanum* belongs to a major late blight R gene cluster on chromosome 4 of potato. *Molecular Plant–Microbe Interactions* 18: 722–729.
- Park TH, Vleeshouwers VGAA, Huigen DJ, van der Vossen EAG, van Eck HJ, Visser RGF. 2005b. Characterization and high-resolution mapping of a late blight resistance locus similar to R2 in potato. *Theoretical and Applied Genetics* 111: 591–597.
- Park TH, Vleeshouwers VGAA, Hutten RCB, van Eck HJ, van der Vossen E, Jacobsen E, Visser RGF. 2005c. High-resolution mapping and analysis of the resistance locus *Rpi-abpt* against *Phytophthora infestans* in potato. *Molecular Breeding* 16: 33–43.
- Pel MA, Foster SJ, Park TH, Rietman H, van Arkel G, Jones JDG, Van Eck HJ, Jacobsen E, Visser RGF, Van der Vossen EA. 2009. Mapping and cloning of late blight resistance genes from *Solanum venturii* using an interspecific candidate gene approach. *Molecular Plant–Microbe Interactions* 22: 601–615.
- Prokhorchik M, Choi S, Chung E-H, Won K, Dangi J, Sohn KH. 2020. A host target of a bacterial cysteine protease virulence effector plays a key role in convergent evolution of plant innate immune system receptors. *New Phytologist* 225: 1327–1342.
- Roux F, Noël L, Rivas S, Roby D. 2014. ZRK atypical kinases: emerging signaling components of plant immunity. *New Phytologist* 203: 713–716.
- Saunders DG, Breen S, Win J, Schornack S, Hein I, Bozkurt TO, Champouret N, Vleeshouwers VG, Birch PR, Gilroy EM *et al.* 2012. Host protein BSL1 associates with *Phytophthora infestans* RXLR effector AVR2 and the *Solanum demissum* Immune receptor R2 to mediate disease resistance. *Plant Cell* 24: 3420–3434.
- Selote D, Kachroo A. 2010. RPG1-B-derived resistance to AvrB-expressing *Pseudomonas syringae* requires RIN4-like proteins in soybean. *Plant Physiology* 153: 1199–1211.
- Seto D, Koulou N, Lo T, Menna A, Guttman DS, Desveaux D. 2017. Expanded type II effector recognition by the ZAR1 NLR protein using ZED1-related kinases. *Nature Plants* 3: 17027.
- Shi X, Long Y, He F, Zhang C, Wang R, Zhang T, Wu W, Hao Z, Wang Y, Wang GL *et al.* 2018. The fungal pathogen *Magnaporthe oryzae* suppresses innate immunity by modulating a host potassium channel. *PLoS Pathogens* 14: e1006878.
- Śliwka J, Jakuczun H, Chmielarz M, Hara-Skrzypiec A, Tomczyńska I, Kilian A, Zimnoch-Guzowska E. 2012a. A resistance gene against potato late blight originating from *Solanum × michoacanum* maps to potato chromosome VII. *Theoretical and Applied Genetics* 124: 397–406.
- Śliwka J, Jakuczun H, Chmielarz M, Hara-Skrzypiec A, Tomczyńska I, Kilian A, Zimnoch-Guzowska E. 2012b. Late blight resistance gene from *Solanum ruizeballoisii* is located on potato chromosome X and linked to violet flower colour. *BMC Genetics* 13: 11.
- Smilde WD, Brigneti G, Jagger L, Perkins S, Jones JD. 2005. *Solanum mochiquense* chromosome IX carries a novel late blight resistance gene *Rpi-moc1*. *Theoretical and Applied Genetics* 110: 252–258.
- Stevenson WR. 1994. The potential impact of field resistance to early blight on fungicide in potato. *American Potato Journal* 71: 317–324.
- Tang M, Ning Y, Shu X, Dong B, Zhang H, Wu D, Wang H, Wang GL, Zhou B. 2017. The Nup98 homolog APIP12 targeted by the effector AvrPiz-t is involved in rice basal resistance against *Magnaporthe oryzae*. *Rice* 10: 5.
- Turnbull D, Wang H, Breen S, Malec M, Naqvi S, Yang L, Welsh L, Hemsley P, Zhendong T, Brunner F *et al.* 2019. AVR2 targets BSL family members, which act as susceptibility factors to suppress host immunity. *Plant Physiology* 180: 571–581.
- Turnbull D, Yang L, Naqvi S, Breen S, Welsh L, Stephens J, Morris J, Boevink PC, Hedley PE, Zhan J *et al.* 2017. RXLR effector AVR2 up-regulates a brassinosteroid-responsive bHLH transcription factor to suppress immunity. *Plant Physiology* 174: 356–369.
- Van Weymers PSM, Baker K, Chen XW, Harrower B, Cooke DEL, Gilroy EM, Birch PRJ, Thilliez GJA, Lees AK, Lynotte JS *et al.* 2016. Utilizing “Omic” technologies to identify and prioritize novel sources of resistance to the oomycete pathogen *Phytophthora infestans* in potato germplasm collections. *Frontiers in Plant Science* 7: 672.
- de Vetten NCMH, Verzaux EC, Vossen JH, Rietman H, Vleeshouwers VGAA, Jacobsen E, Visser RGF. 2014. Cloning and exploitation of a functional R-gene from *Solanum × edinense*. US patent 20140041072 A1.
- Vleeshouwers VG, Raffaele S, Vossen JH, Champouret N, Oliva R, Segretin ME, Rietman H, Cano LM, Lokossou A, Kessel G *et al.* 2011. Understanding and exploiting late blight resistance in the age of effectors. *Annual Review of Phytopathology* 49: 507–531.
- Vossen JH, Nijenhuis M, Arens-de Reuver MJB, van der Vossen EAG, Jacobsen E, Visser RGF (2009). Cloning and exploitation of a functional R gene from *Solanum chacoense*. US patent WO 2011034433 A1.

Wang G, Roux B, Feng F, Guy E, Li L, Li N, Zhang XJ, Lautier M, Jardinaud M, Chabannes M *et al.* 2015. The decoy substrate of a pathogen effector and a pseudokinase specify pathogen-induced modified-self recognition and immunity in plants. *Cell Host & Microbe* 18: 285–295.

Wang J, Hu M, Wang J, Qi J, Han Z, Wang G, Qi Y, Wang HW, Zhou JM, Chai JJ. 2019a. Reconstitution and structure of a plant NLR resistosome conferring immunity. *Science* 364: eaav5870.

Wang J, Wang J, Hu M, Wu S, Qi J, Wang G, Han Z, Qi Y, Gao N, Wang H *et al.* (2019b). Ligand-triggered allosteric ADP release primes a plant NLR complex. *Science* 364: eaav5868.

Wang R, Ning Y, Shi X, He F, Zhang C, Fan J, Jiang N, Zhang Y, Zhang T, Hu Y *et al.* 2016. Immunity to rice blast disease by suppression of effector-triggered necrosis. *Current Biology* 26: 2399–2411.

Supporting Information

Additional Supporting Information may be found online in the Supporting Information section at the end of the article.

Fig. S1 Protein sequence alignment of R2 and Rpi-mcq1.

Fig. S2 Representative hypersensitive response (HR) scoring scale images.

Fig. S3 Protein sequence alignment of *Nicotiana benthamiana* (Nb) and potato (St) BSL1 (a) and BSL2 and BSL3 (b).

Fig. S4 Transcript expression of *NbBSLs* and protein stability of PiAVR2, R2 and Rpi-mcq1 in *NbBSL*-silenced plants.

Fig. S5 Protein stability of PiAVR2, R2 and Rpi-mcq1 when co-expressed with StBSLs in *N. benthamiana*.

Fig. S6 PiAVR2 interacts with StBSL1, StBSL2 and StBSL3, but no direct interaction of R2 or Rpi-mcq1 with StBSLs or PiAVR2 was observed.

Fig. S7 Interaction of R2 with StBSL1 is dependent on PiAVR2.

Fig. S8 Interaction of R2 with NbBSL1 is dependent on PiAVR2, with no observable interaction between NbBSLs and Rpi-mcq1.

Fig. S9 GFP-BSL fusion proteins are stable in the presence of the phosphatase inhibitor okadaic acid (OA).

Fig. S10 Protein stability of PiAVR2, R2 and Rpi-mcq1 after okadaic acid treatment.

Fig. S11 Phosphatase activity is abolished in BSL phosphatase-dead (PD) mutants.

Fig. S12 Protein stability of PiAVR2, R2 and Rpi-mcq1 when co-infiltrated with wild-type (WT) or PD StBSLs in *N. benthamiana*.

Fig. S13 Interaction between WT and PD StBSLs.

Table S1 Details of primers used in this study.

Please note: Wiley Blackwell are not responsible for the content or functionality of any Supporting Information supplied by the authors. Any queries (other than missing material) should be directed to the *New Phytologist* Central Office.